IEEE Journal of Oceanic Engineering 31(4):922-934, 2006

Formation Control of Marine Surface Craft: A Lagrangian Approach

Ivar-André F. Ihle, Jérôme Jouffroy and Thor I. Fossen

***Abstract*—This paper presents a method for formation control of marine surface craft inspired by Lagrangian mechanics. The desired formation configuration and response of the marine surface craft are given as a set of constraint functions. The functions are treated according to constraints in analytical mechanics. Thus, constraint forces arise and feedback from the constraint functions keeps the formation assembled. Since the constraint functions are designed for a desired effect, the forces can be interpreted as control laws. Examples of constraint functions that maintain a formation are presented. Furthermore, the same approach has been applied with no major modification to position control purposes for a single vessel. An extension to underactuated vessels is given. Simulations with nonlinear models of tugboats illustrate the proposed method versatility and its robustness with respect to environmental disturbances and time delays.**

***Index Terms*—Analytical mechanics, formation control, marine surface vessels.**

I. Introduction

THE fields of coordination and formation control with applications towards mechanical systems, ships, aircraft, unmanned vehicles, spacecraft, etc., have been the object of increased research interest in recent years. This interest has gained momentum due to technological advances in the development of powerful control techniques for single vehicles, the increasing computational and communication capabilities, and the ability to create small, low-power, low-cost systems. Researchers have also been motivated by group behaviors in nature, such as flocking and schooling, which benefits the animals in the formation [1]–[4]. Many models from biology have been developed to give an understanding of the traffic rules that govern fish schools, bird flocks, and other animal groups, which again have provided motivation for control synthesis and computer graphics (see [5], [6], and the references therein).

Some of the reasons for considering the use of distributed vehicles are their characteristics of structural flexibility, reliability through redundancy, increased instrument resolution, and reduced cost, since several simple, inexpensive systems can compete with singular sophisticated and expensive systems, and it is expected that a cooperative mobile network of sensors can outperform a single large vehicle with multiple sensors, when the goal is to climb the gradient of an environmental field [7]. Marine applications include icebreaker escort, underway replenishment, and tandem loading, where motions are coordinated to avoid collisions. An additional motivation for marine surface craft is reduced drag forces. Autonomous ocean sampling networks have attracted wide interest (see, e.g., [8]). In these applications, communication constraints and environmental disturbances pose challenges for control design [9].

There exists a large number of publications in the fields of cooperative and formation control of autonomous vehicles—recent results can be found in [4], [7], [10]–[12], and references therein. While the applications are different, some common fundamental parts can be extracted from the many existing approaches to vehicle formation control. Roughly, three approaches are found in the literature: leader-following, behavioral methods, and virtual structures.

Briefly explained, the leader-following architecture defines a leader in the formation while the other members of the formation follow that leader [13], [14]. The behavioral approach prescribes a set of desired behaviors for each member in the group, and weighs them such that desirable group behavior emerges. Possible behaviors include trajectory and neighbor tracking, collision and obstacle avoidance, and formation keeping [15].

In the virtual structure approach, the entire formation is treated as a single, virtual, structure. Formation control of virtual structures has been achieved, e.g., by making all members of the formation track assigned nodes which move through space in the desired configuration, and then use formation feedback to prevent members from leaving the formation [16]. In [17], each member of the formation tracks a virtual element at the same time as the motion of the elements is governed by a function that specifies the desired geometry of the formation.

Control laws for redundant robotic manipulator control [18] have been extended to formation control, and incorporate parts of the aforementioned approaches. The extension was originally proposed in [19] where task functions describe formation behaviors and inverse kinematics is used to assign task priority. The authors of [20] extend the result by using singularity-robust inverse kinematics.

Coordinated control applications for marine surface vessels have been investigated for low-speed replenishment operations [21], [22], and also for a surface craft following an underwater vehicle [14]. For surface vessels, it is relatively easy to communicate using radio-frequency technology. However, a decentral-

I.-A. F. Ihle and J. Jouffroy are with the Centre for Ships and Ocean Structures (CeSOS), Norwegian University of Science and Technology (NTNU), Trondheim NO-7491, Norway (e-mail: ihle@ntnu.no; jouffroy@ntnu.no).

T. I. Fossen is with the Centre for Ships and Ocean Structures (CeSOS) and the Department of Engineering Cybernetics, Norwegian University of Science and Technology NTNU, Trondheim NO-7491, Norway (e-mail:fossen@ieee.org).

ized control law implementation is desirable due to safety issues such as breakdown of communication channels and redundancy reliability. Position is measured with either local or global navigation systems (or a combination). Local position reference systems include taut-wire, hydroacoustic, and laser measurements. Among the commercially available global navigation satellite systems the American system called Navstar global positioning system (GPS) is one of the most popular. Advanced vessels also frequently incorporate an inertial navigation system. In addition, an observer is used to filter out high-frequency wave-motion components and estimate nonmeasured body velocities.

This paper investigates how tools from analytical mechanics [23] can be used for formation control of marine surface craft. A collection of independent bodies/vehicles are controlled as a formation by employing functions that describe a vehicles behavior with respect to other vehicles position and velocity. By treating these functions as mechanical constraints in an analytical setting, control laws that maintain the formation structure emerge. In this way, the coordinated movement of the formation is decided by forces that maintain the given functions at all times. The proposed framework incorporates physical modelling issues as well as control objectives and is not necessarily restricted to formation control. Preliminary results were reported in [24].

Mechanical constraint forces, which cause the bodies to act in accordance with the constraints, are well known from the early days of analytical mechanics [25] and have been used with success, e.g., in computer graphics applications [26], [27] and robotics [28] The main idea in this paper is to show how constraint functions impose constraint forces which maintain the configuration of a formation as a virtual structure. The formation is also maintained when some, or all, of the members are exposed to external forces, measurement noise, or delays in the communication channels. The same approach can be used for constructing control laws for specific tasks, e.g., point stabilization or trajectory tracking, which can be combined with the control laws that maintain the formation structure. Together, the constraint functions form control laws that both govern the movement of the entire formation and perform a specific task given by the imposed constraint function(s).

The rest of this paper is organized as follows. Section II presents a model for a formation of marine surface vessels with constraints and methods for stabilizing constraints. Examples of constraint functions for formation control and other control purposes are also given. Comments on decentralized communication and implementation and an extension to underactuated vessels are given in Section III. Section IV presents case studies of formation control of marine craft with constraints, and Section V contains some concluding remarks.

II. Modeling, Control, and Constraints

Example 1 (Formation Assembling): To motivate and introduce the main idea of the method given in this section and illustrate how the constraint function affects the motion of independent systems, we look at a formation of two point masses $\eta_1, \eta_2 \in \mathbb{R}^2$, with kinetic energy $\mathcal{T} = (1/2)\dot{\eta}^\top M\dot{\eta}$, where $\eta = \left[\eta_1^\top, \eta_2^\top\right]^\top$ and $M = M^\top > 0$ is the mass matrix; $M = \operatorname{diag}(m_1 I_2, m_2 I_2)$ where I_2 denotes the 2×2-identity matrix. The goal for the formation is to let the two members operate at a specified length away from each other. When their positions violate the specified length, the masses should move such that this length is rectified. This distance requirement between the points can be formulated as the constraint function

$$\mathcal{C}(\eta) = (\eta_1 - \eta_2)^\top(\eta_1 - \eta_2) - r^2 = 0 \tag{1}$$

where $r > 0$ is the desired distance between η_1 and η_2. The procedure in Section III gives the following equation of motion when (1) is satisfied:

$$M\ddot{\eta} = \tau - W(\eta)^\top\lambda \tag{2}$$

where $W(\eta)$ is the Jacobian of the constraint function (1), λ is the corresponding Lagrangian multiplier with stabilizing feedback from the constraints, and τ is the external forces. If the system has initial conditions that violate the constraint (1), the masses converge such that (1) is met. When τ in (2) is zero for all time, the system will converge to a position between the initial positions of η_1 and η_2 where the distance between η_1 and η_2 is r. If both masses are initially perturbed with a small amount of force, the motion of the masses will still satisfy the constraint function. As seen in Fig. 1, the masses move such that constraint (1) is satisfied—they *assemble* into a formation defined by the constraint function.

A. System Modeling

Consider n systems each of order m with kinetic and potential energy $\mathcal{T}_i$ and $\mathcal{U}_i$, respectively. The Lagrangian of the total system is then

$$\mathcal{L} = \mathcal{T} - \mathcal{U} = \sum_{i=1}^{n} \mathcal{T}_i - \mathcal{U}_i.$$

There exist kinematic relations

$$\mathcal{C}(\eta) = 0 \quad \mathcal{C}(\eta) \in \mathbb{R}^p \tag{3}$$

between the coordinates which restrict the state space to a constraint manifold $\mathcal{M}_c$ with less than $2n \cdot m$ dimensions. We denote $\mathcal{C}(\eta)$ the *constraint function*, where $\eta \in \mathbb{R}^{nm}$ contains the generalized positions $\eta_1, \ldots, \eta_n$. We know from [23] that the forces that maintain the kinematic constraints add potential energy to the system

$$\bar{\mathcal{U}} = \mathcal{U} + \lambda^\top\mathcal{C}(\eta)$$

which gives the modified Lagrangian

$$\bar{\mathcal{L}} = \mathcal{T} - \mathcal{U} - \lambda^\top\mathcal{C}(\eta)$$

where $\lambda \in \mathbb{R}^p$ is the Lagrangian multiplier(s). To obtain the equations of motion, we apply the Euler–Lagrange differential equations with auxiliary conditions for $i = 1, \ldots, nm$

$$\begin{aligned} \frac{d}{dt}\frac{\partial\mathcal{L}}{\partial\dot{\eta}_i} - \frac{\partial\mathcal{L}}{\partial\eta_i} + \lambda^\top\frac{\partial\mathcal{C}(\eta)}{\partial\eta_i} + \left(\frac{\partial\lambda}{\partial\eta_i}\right)^\top\mathcal{C}(\eta) &= \tau_i \\ \mathcal{C}(\eta) &= 0 \end{aligned}$$

which implies

$$\frac{d}{dt}\frac{\partial\mathcal{L}}{\partial\dot{\eta}_i} - \frac{\partial\mathcal{L}}{\partial\eta_i} = \tau_i - \lambda^\top\frac{\partial\mathcal{C}(\eta)}{\partial\eta_i} \tag{4}$$

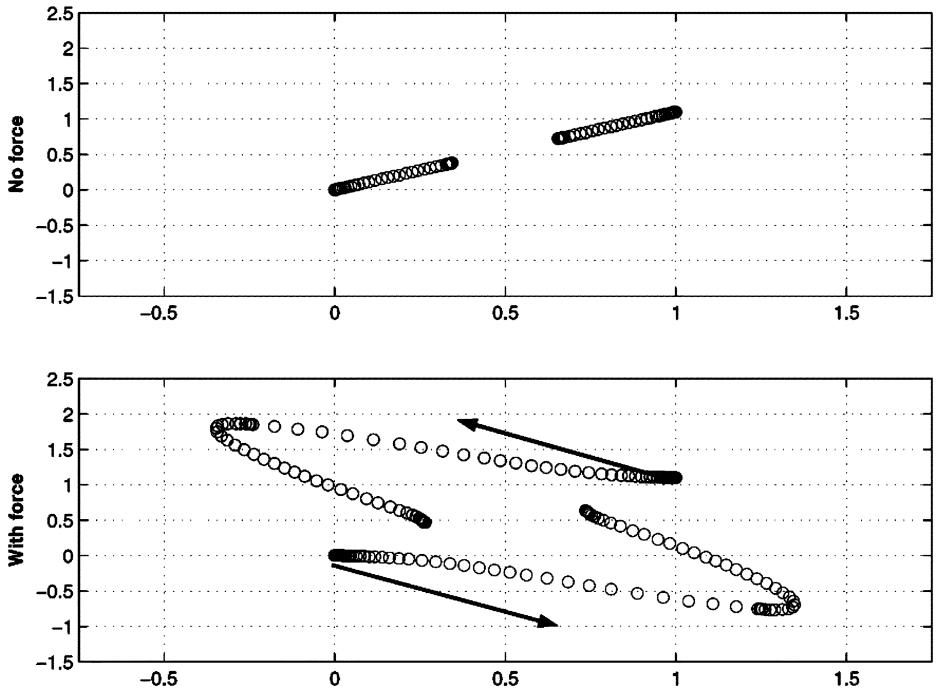

Fig. 1. Position plot of η_1 and η_2—starts in (0,0) and (1,1), respectively. $r = 0.5$. The lower part includes the initial force disturbances shown as arrows.

where τ_i is the generalized external force associated with coordinate η_i.

Equation (3) constrains the systems motion to a subset, $\mathcal{M}_c \subseteq \mathbb{R}^{2nm-p}$ of the state space where $\mathcal{C}(\eta) = 0$. Since we want to keep the systems on $\mathcal{M}_c$, neither the velocity nor the acceleration should violate the constraints. To find the velocities that correspond to (3), the kinematic admissible velocities, the constraint function is differentiated with respect to time. Similarly, we differentiate twice to find the acceleration of the constraints. This gives the additional conditions

$$\begin{aligned} \dot{\mathcal{C}}(\eta) &= W(\eta)\dot{\eta} = 0 \\ \ddot{\mathcal{C}}(\eta) &= W(\eta)\ddot{\eta} + \dot{W}(\eta)\dot{\eta} = 0 \end{aligned} \tag{5}$$

where $W(\eta) \in \mathbb{R}^{mn \times p}$ is the Jacobian of the constraint function, i.e., $W(\eta) = (\partial \mathcal{C}(\eta)/\partial \eta)$. An expression for the Lagrangian multiplier is found by obtaining an expression for $\ddot{\eta}$ in (4) and inserting it into (5).

An expression for the forces that maintain the constraints, the constraint forces, is found from the right-hand side of (4)

$$\tau_{\text{constraint}} = -\left(\frac{\partial \mathcal{C}(\eta)}{\partial \eta}\right)^{\top} \lambda = -W(\eta)^{\top}\lambda.$$

The forces can also be found from the principle of virtual work [23, Ch. III.5]: The gradient $W(\eta)$ is normal to the constraint $\mathcal{C}(\eta) = 0$, and since the forces between independent bodies that maintain a kinematic constraint (equilibrium) are required to do no virtual work, we have

$$\tau_{\text{constraint}} \cdot \dot{\eta} = 0 \qquad \forall\, \eta | W(\eta)\dot{\eta} = 0. \tag{6}$$

Hence, the constraint force must be a linear combination of the columns in $W(\eta)$

$$\tau_{\text{constraint}} = -\left(\frac{\partial \mathcal{C}(\eta)}{\partial \eta}\right)^{\top} \lambda. \tag{7}$$

The Lagrangian multiplier is then found by combining the equations of motion with the constraint acceleration. It is clear that the Lagrangian λ term provides the force of reaction which maintains the kinematic constraint [23].

The main focus in this paper is marine craft,[1] so we introduce the equation of motion for a single marine vessel in the body-fixed frame, derived in [29]

$$\begin{aligned} \dot{\eta} &= R(\psi)\nu \\ M\dot{\nu} + C(\nu)\nu + D(\nu)\nu + g(\eta) &= \tau \end{aligned}$$

where $\eta = [x, y, \psi]^{\top}$ is the Earth-fixed position vector, (x, y) is the position on the ocean surface, ψ is the heading angle (yaw), and $\nu = [u, v, r]^{\top}$ is the body-fixed velocity vector. The model matrices M, C, and D denote inertia, Coriolis plus centrifugal, and damping, respectively, while g is a vector of generalized forces and

$$R(\psi) = \begin{bmatrix} \cos\psi & -\sin\psi & 0 \\ \sin\psi & \cos\psi & 0 \\ 0 & 0 & 1 \end{bmatrix}$$

is the rotation matrix between the body and the inertial Earth coordinate frame. It has the properties that $R(\psi)^{\top} R(\psi) = I$ and $\|R(\psi)\| = 1$ for all ψ, and $(d/dt)R(\psi) = R(\psi)S\dot{\psi}$ where

$$S = \begin{bmatrix} 0 & -1 & 0 \\ 1 & 0 & 0 \\ 0 & 0 & 0 \end{bmatrix} = -S^{\top}$$

is skew-symmetric. For more details regarding ship modeling, the reader is advised to consult [29]. Next, consider a formation of n vessels with position given by η_i, inertia matrix M_i, and so on for $i = 1, \ldots, n$. We collect the vectors into new vectors,

[1]Note that this approach is also valid for mechanical systems such as $M(q)\ddot{q} + C(q, \dot{q})\dot{q} = \tau$ (robot manipulator).

and the matrices into new, block-diagonal matrices by defining $\eta = \left[\eta_1^\top, \ldots, \eta_n^\top\right]^\top$ and $M = \mathrm{diag}\{M_1, \ldots, M_n\}$, and similarly for the other vectors and matrices. Assume that there are constraint functions on the position between the ships, corresponding to the case in (4). The addition of the potential energy from the constraints gives

$$\dot{\eta} = R(\psi)\nu \tag{8a}$$
$$M\dot{\nu} + C(\nu)\nu + D(\nu)\nu + g(\eta) = \tau_{\mathrm{env}} + \tau_{\mathrm{constraint}} \tag{8b}$$
$$\mathcal{C}(\eta) = 0 \tag{8c}$$

where

$$\tau_{\mathrm{constraint}} = -\left(\frac{\partial \mathcal{C}(\eta)}{\partial \eta}\right)^\top \lambda = -W(\eta)^\top \lambda$$

is the expression for the constraint forces which maintain the constraint function (8c).

A vessel i is a neighbor with a vessel j if they share each other's information. In our setting, vessels are neighbors if they appear in the same constraint function. Given a set of constraint functions $\mathcal{C}(\eta) = [\ldots, \mathcal{C}_k(\eta), \ldots]^\top$ with corresponding Lagrangian multipliers $\lambda = [\ldots, \lambda_k, \ldots]^\top$, the resulting constraint forces for an individual ship i are

$$\tau_{\mathrm{constraint},i} = \sum_{k \in \mathcal{A}_c} -\left(\frac{\partial \mathcal{C}_k(\eta)}{\partial \eta_i}\right)^\top \lambda_k = \sum_{k \in \mathcal{A}_c} -W_{ki}^\top \lambda_k \tag{9}$$

where $\mathcal{A}_c$ is the set of indices where constraint functions with η_i appear and $W_{ki} = 0$ for $k \notin \mathcal{A}_c$.

The equation of motion is transformed to the Earth-fixed frame by the kinematic transformation in [29, Ch. 3.3.1] which results in

$$M_\eta(\eta)\ddot{\eta} + n(\nu, \eta, \dot{\eta}) = \tau_\eta - R(\psi)W(\eta)^\top \lambda \tag{10}$$

where

$$\begin{aligned}
n(\nu, \eta, \dot{\eta}) &= C_\eta(\nu, \eta)\dot{\eta} + D_\eta(\nu, \eta)\dot{\eta} + g_\eta(\eta) \\
M_\eta(\eta) &= R(\psi) M R(\psi)^\top \\
C_\eta(\nu, \eta) &= R(\psi)[C(\nu) - M R(\psi)^\top \dot{R}(\psi)] R(\psi)^\top \\
D_\eta(\nu, \eta) &= R(\psi) D(\nu) R(\psi)^\top \\
g_\eta(\eta) &= R(\psi) g(\eta) \\
\tau_\eta &= R(\psi)\tau_{\mathrm{env}}.
\end{aligned}$$

The combination of (5) and (10) gives a differential algebraic equation (DAE). Solving for $\ddot{\eta}$ and substituting gives (the arguments have been removed to ease the presentation)

$$W M_\eta^{-1} R W^\top \lambda = W M_\eta^{-1}\{\tau_\eta - n\} + \dot{W}\dot{\eta}. \tag{11}$$

Then, (10) with (11) for λ give the equation of motion for the systems subject to (3).

Assumption 1: The mass matrix M is positive definite, i.e., $M = M^\top > 0$, hence $M_\eta(\eta) = M_\eta(\eta)^\top > 0$ since $R(\psi)$ is orthogonal.

Assumption 2: The constraint function (3) has a unique equilibrium. The Jacobian $W(\eta)$ has full row-rank, i.e., the constraints are not conflicting or redundant, and is limited by a linear growth-rate condition, e.g., $k_1 |\eta| \leq |W| \leq k_2 |\eta|$.

Note that redundant or conflicting constraints arise when one or more rows (columns) in $\mathcal{C}$ are a linear combination of other rows (columns), or when the functions are contradicting. An example would be the same constraint function appearing twice in $\mathcal{C}(\eta)$.

Assumptions 1 and 2 guarantee that $W M_\eta^{-1} R W$ exists since M_η is positive definite, hence M_η^{-1} exists and $W M_\eta^{-1} R W^\top$ is nonsingular. Thus, the expression can be solved for λ and used in (10).

B. Stabilization of Constraint Functions

If the system starts on the constraint manifold $\mathcal{M}_c$, that is, the initial conditions $\eta(0)$ and $\dot{\eta}(0) = (\eta_0, \dot{\eta}_0)$ satisfy $(\eta_0, \dot{\eta}_0) \in \mathcal{M}_c$ such that

$$\mathcal{C}(\eta_0) = 0 \quad \text{and} \quad \dot{\mathcal{C}}(\eta_0) = 0$$

and the force τ does not perturb the system, then the solution is $(\eta(t), \dot{\eta}(t)) \in \mathcal{M}_c$ for all times. However, if the initial conditions are not in $\mathcal{M}_c$, or the system is perturbed subject to $(\eta, \dot{\eta}) \notin \mathcal{M}_c$, feedback must be used to stabilize the constraint.

We want to investigate stability of the constraint, that is, we look at stability of

$$\mathcal{M}_c = \{(\eta, \dot{\eta}) : \mathcal{C}(\eta) = 0,\ W(\eta)\dot{\eta} = 0\}.$$

Consider the case when $\tau \neq 0$ in (10), and suppose that $(\eta_0, \dot{\eta}_0) \notin \mathcal{M}_c$. If we use the equations from Section II-A, then

$$\ddot{\mathcal{C}}(\eta) = 0 \tag{12}$$

which is unstable—when $\mathcal{C}(\eta)$ is a scalar function, its transfer function contains two poles at the origin. Hence, if $\mathcal{C}(\eta) = 0$ is not fulfilled initially, the solutions might blow up in finite time. Even if $\mathcal{C}(\eta_0) = 0$, this can happen if there is a measurement noise on η. This instability is, in fact, an inherent property of higher index DAEs [30], and is one of the reasons numerical methods for differential-algebraic equations have received special attention [31], e.g., in modelling of mechanical systems [32].

This can be solved by using feedback from the constraints in the expression for the Lagrangian multiplier (11)

$$\begin{aligned}
W M_\eta^{-1} R W^\top \lambda = W M_\eta^{-1}\{\tau_\eta - n\} \\
+ \dot{W}\dot{\eta} + K_d \dot{\mathcal{C}}(\eta) + K_p \mathcal{C}(\eta)
\end{aligned} \tag{13}$$

where $K_p, K_d \in \mathbb{R}^{p \times p}$ are positive definite. The constraint force for vessel i is given by

$$\begin{aligned}
\tau_{\mathrm{constraint},i} = \sum_{k \in \mathcal{A}_c} \sum_{j \in \mathcal{C}_k} -W_{ki}^\top \left(W_k M_{\eta,ij}^{-1} R_{ij} W_k^\top\right)^{-1} \\
\times \left\{W_{ki} M_{\eta,ij}(\tau_{\eta,ij} - n_{ij}) + k_d \dot{\mathcal{C}}_k + k_p \mathcal{C}_k\right\}
\end{aligned}$$

where the subscript ij represents a block-diagonal matrix A_{ij} with blocks A_i and A_j, or an augmented column vector $a_{ij} := \left[a_i^\top, \alpha_j^\top\right]^\top$ and is an essential information about i and

its neighbor j. When we add the stabilizing terms, we consider a stabilized version of (12)

$$\ddot{\mathcal{C}} = -K_d\dot{\mathcal{C}}(\eta) - K_p\mathcal{C}(\eta) \tag{14}$$

which ensures that $\mathcal{C}(\eta)$ and $\dot{\mathcal{C}}(\eta)$ tend to zero.

We rewrite (14) using

$$\phi_1(t) = \mathcal{C}(\eta(t)) \quad \phi_2(t) = \dot{\mathcal{C}}(\eta(t)) \quad \phi = \begin{bmatrix} \phi_1 \\ \phi_2 \end{bmatrix}$$

such that

$$\begin{bmatrix} \dot{\phi}_1 \\ \dot{\phi}_2 \end{bmatrix} = \begin{bmatrix} 0 & I \\ -K_p & -K_d \end{bmatrix} \begin{bmatrix} \phi_1 \\ \phi_2 \end{bmatrix} \quad \text{or} \quad \dot{\phi} = A\phi. \tag{15}$$

By appropriate choice of K_p and K_d, A is Hurwitz. Then, by choosing a design matrix $Q = Q^\top > 0$, we find a $P = P^\top > 0$ such that

$$PA + A^\top P = -Q.$$

Then, from

$$V(\phi) = \phi^\top P\phi > 0 \qquad \forall\, \phi \neq 0 \tag{16}$$

$$\dot{V}(\phi) = -\phi^\top Q\phi < 0 \qquad \forall\, \phi \neq 0 \tag{17}$$

the set $\mathcal{M}_c$ is a globally exponentially stable set of equilibrium points of the system

$$\begin{aligned} M_\eta(\eta)\ddot{\eta} + n(\nu, \eta, \dot{\eta}) &= -R(\psi)W(\eta)^\top\lambda \\ \mathcal{C}(\eta) &= 0 \end{aligned} \tag{18}$$

under Assumptions 1 and 2 [33].

By applying feedback from the constraints and converting (12) to (14), the formation is stabilized when the initial values do not fulfill the constraint function.

Remark 1: Consider the case in Example 1 and set $K_p = \beta^2$ and $K_d = 2\alpha$, such that $\ddot{\mathcal{C}} + 2\alpha\dot{\mathcal{C}} + \beta^2\mathcal{C} = 0$, $\alpha,\ \beta > 0$. In the numerical scientific community, this is referred to as the Baumgarte stabilization technique [34], used for stabilization of numerical simulations of multibody and constrained systems and DAEs.

There exists a wide number of numerical methods that stabilize DAEs (see [35] and references therein). Applying feedback, such as in (14), is intuitive and familiar from a control point of view, which serves as a motivation for this approach

C. Constraint Functions for Control Purposes

So far the focus has been on systems with constraints in general without addressing how the constraint functions arise. In the control literature, the main focus has been on constrained robot manipulators with physical contact between the end effector and a constraint surface. This occurs in many tasks, including scribing, writing, grinding, and others as described in [36], [37], and references therein. These constraints are inherently in the system as they are all based on how the model or the environment constrains the dynamics. Some of the difficulties related to simulations of constrained systems and ways to solve them are presented in [38].

However, if a control objective is defined as a constraint function and if these *constraints are imposed* on the system, the framework for stabilization of constraints described in Section II-B can be used to design control laws. In this way, the control law forces the system to behave according to the constraint function. As an example, consider stabilization of a point mass to a desired location.

Example 2 (Point Stabilization): Consider a single point mass subject to the constraint

$$\mathcal{C}(\eta) = \eta = 0, \qquad \eta \in \mathbb{R}$$

but not exposed to any external forces, i.e., $\tau = 0$

$$m\ddot{\eta} = -W(\eta)\lambda$$

where $W(\eta) = 1$, $m = 1$, and λ are given as in (13)

$$\lambda = 2\alpha\dot{\eta} + \beta^2\eta, \qquad \alpha, \beta \in \mathbb{R}.$$

The constraint manifold is now the origin, i.e., $\mathcal{M}_c = (0, 0)$, and the dynamics are

$$\ddot{\eta} = -2\alpha\dot{\eta} - \beta^2\eta$$

which is shown to be globally exponentially stable for $\alpha, \beta > 0$. Given an initial condition $(\eta(0), \dot{\eta}(0)) \notin \mathcal{M}_c$, the trajectory $\eta(t)$ converges exponentially to the origin. In this case, the constraint function corresponds to a proportional-derivative (PD) controller. This approach for control design, and its combination with formation constraints, will be explained further in Section II.

To avoid a Jacobian with less than full rank, which again leads to singularities in (13), Assumption 2 yields no redundant constraints to be imposed on the system. Thus, no singular positions are encountered. However, if one situation with redundant constraints should arise, singularities have to be avoided. The problem of kinematic singularities has been intensively studied in robotics, and one strategy is the damped least-squares (DLS) technique [39], [40]. The method corresponds to instead of solving (13) as $\lambda = A_1^{-1}b$, where $A_1(\eta) = W(\eta)M_\eta^{-1}(\eta)R(\psi)\,W(\eta)^\top$ and b is the right-hand side of (13); the equation is written as $A_2(\eta)W(\eta)^\top\lambda = b$ which is solved by

$$A_2(\eta)^\top b = \left(A_2(\eta)^\top A_2(\eta) + \gamma I\right) W(\eta)^\top\lambda \tag{19}$$

where $\gamma \geq 0$ is the damping factor. When $\gamma = 0$ the solution of (19) corresponds to the solution of (13). The damping factor must be selected carefully: small values give accurate solutions but decreased robustness to singularities. The solution of (19) is

$$W(\eta)^\top\lambda = \left(A_2(\eta)^\top A_2(\eta) + \gamma I\right)^{-1} A_2(\eta)^\top b.$$

The DLS technique permits a wider combination of constraint functions, which could cause singularities in the solution otherwise, and allows a set of redundant constraint functions to be used. Consequently, the DLS method relaxes the assumption on the Jacobian.

D. Different Types of Constraints

To explain how formation control is achieved, this section will consider some examples of imposed constraints that coordinate and control certain aspects of the group behavior. Dif-

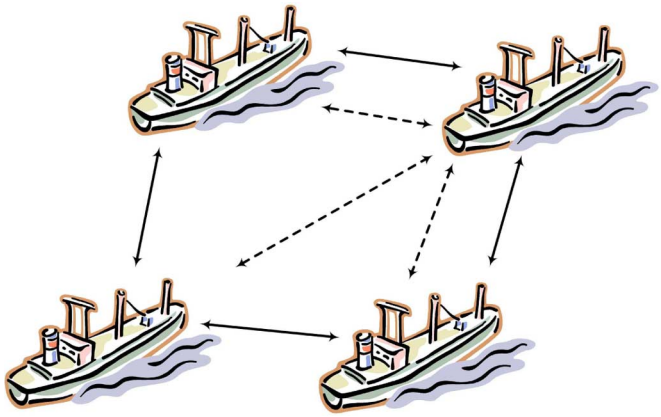

Fig. 2. Different constraint functions acting between vessels determine collective motion. Two types of constraint functions are illustrated: $\mathcal{C}_{rd}(\ \text{—}\ )$ and $\mathcal{C}_{fd}(\ \text{- - -}\ )$.

ferent formation configurations are useful during changing operations, such as collision avoidance, seabed scanning, etc. To keep the notation compact, η_i and $\dot{\eta}_i$ are used for position and velocity of vehicle i, and collected into vector notation as $\eta = \left[\eta_1^\top, \ldots, \eta_n^\top\right]^\top$ and $\dot{\eta} = \left[\dot{\eta}_1^\top, \ldots, \dot{\eta}_n^\top\right]^\top$. An illustration of different types of constraint functions is shown in Fig. 2.

1) Distance Between Members: To keep a fixed distance between members of the formation, functions arising from mathematical norms are applied. To maintain a relative distance r_{ij} between group members i and j, let the function be defined by

$$\mathcal{C}_{rd}(\eta) = (\eta_i - \eta_j)^\top(\eta_i - \eta_j) - r_{ij} = 0, \qquad r_{ij} \in \mathbb{R}. \quad (20)$$

This was used in Example 1. If the control objective implies a stricter formation, with fixed offsets in the direction of each coordinate axis, consider the alternative distance function

$$\mathcal{C}_{fd}(\eta) = \eta_i - \eta_j - o_{ij} = 0, \qquad o_{ij} \in \mathbb{R}^m \quad (21)$$

where o_{ij} describes the offset between members i and j.

Furthermore, a set of distance constraint functions defines the entire formation structure. For example, two vehicles with one $\mathcal{C}_{rd}$-function is a line-formation, three vehicles with two $\mathcal{C}_{rd}$-functions form a triangle, and so on. By using $\mathcal{C}_{fd}$, constraints can also be imposed on the orientation, and the desired offset between two members can be limited to a certain coordinate axis. The last approach can be utilized in a formation of autonomous underwater vehicles (AUVs) moving on a horizontal plane. Different constraint functions can be obtained by using body-fixed coordinates.

2) Position Constraints: As shown in Example 2, constraint functions must not necessarily be imposed between independent bodies. A vehicle i is constrained to a single stationary point $\eta_d \in \mathbb{R}^m$ with the following function:

$$\mathcal{C}_p(\eta_i) = \eta_i - \eta_d = 0. \quad (22)$$

This approach can be extended by considering a time-dependent point

$$\mathcal{C}_{tt}(\eta_i, t) = \eta_i - \eta_d(t) = 0 \quad (23)$$

where $q_d(t)$ now represents a path parameterized by time and at least three times differentiable with respect to time. This has now evolved into a trajectory-tracking problem for vehicle i. The addition of the time variable in the constraint function leads to a different expression for constraint velocity and acceleration, but the procedure to find the Lagrange multiplier is straightforward. Note that the expression for the constraint forces remains the same in this case, i.e., $\tau_{\text{constraint}} = -W^\top\lambda$.

3) Combined Constraints: The position constraint is easy to combine with other constraints: Let $W_{rd}^\top\lambda_{rd}$ and $W_p^\top\lambda_p$ be forces that arise from $\mathcal{C}_{rd}$ and $\mathcal{C}_p$. Then, the combination

$$W^\top\lambda = \begin{bmatrix} W_{rd}^\top & W_p^\top \end{bmatrix} \begin{bmatrix} \lambda_{rd} \\ \lambda_p \end{bmatrix}$$

will give constraint forces that regulate the formation in accordance to both (20) and (22).

4) Formation Average Position: A constraint function that express the mean value of all vehicles compared to a desired position for the formation's location is given by [19], [20]

$$\mathcal{C}_a(\eta, t) = \left\{\frac{1}{n}\sum_{i=1}^{n}\eta_i\right\} - \eta_d(t) = \bar{\eta} - \eta_d(t) = 0 \quad (24)$$

where $\bar{\eta}$ is the average position. The time-dependent variable η_d is simply a reference trajectory for the desired location of the formation. This function is of higher interest when it is combined with the following.

5) Formation Variance: As an alternative to control a formation as a rigid structure, the variance of the formation together with the average position can regulate the spreading of the vehicles around that position. The constraint function is given by

$$\mathcal{C}_v(\eta) = \frac{1}{n}\sum_{i=1}^{n}(\eta_i - \bar{\eta})^2 - \text{var}_d = 0 \quad (25)$$

where var_d is the desired variance around the average position $\bar{\eta}$. However, controlling the formation variance does not guarantee that all vehicles stay apart or within a bounded area of the average position, and may lead to unsafe motion.

III. Discussion

The motivation for using constraint functions to achieve formation control lies in the possibility of relating them with constraints in analytical mechanics which have been well known for a long time. Furthermore, and contrary to [28], where the analytical mechanics paradigm is also used as a starting point, the same methods that are necessary to numerically stabilize the constraints in simulations are used to stabilize a constraint manifold.

The previous design, where constraint functions formulated as the control objectives are put into vector form, gives control laws that regulate the entire formation. Combined with control laws for single vehicles in the formation, the design ends up with a closed-loop system that behaves according to the given constraint functions. Moreover, stability and convergence to the constraint manifold is guaranteed by the feedback from the constraint. Hence, a control scheme which incorporates several different formation behaviors with other control laws and guarantees stability has been achieved.

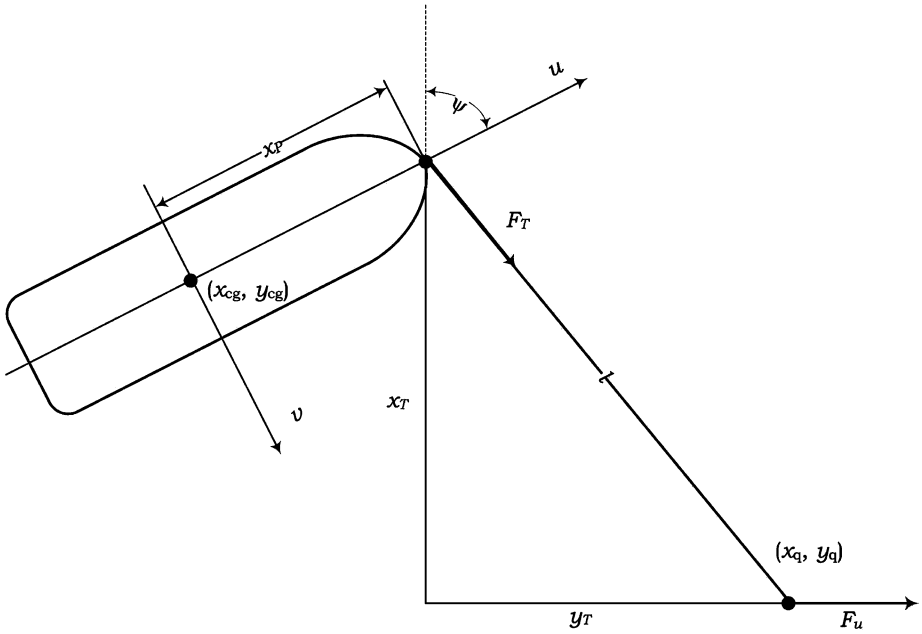

Fig. 3. Point mass and underactuated vessel.

A. Communication Requirements

In the same setting as Section II-D, consider now a formation with a ring-structure where the set $\mathcal{A}_c = \{i, i+1\}$ for $i = 2, \ldots, n-1$, that is, the position of vehicle i appears in constraint functions, as in (20)

$$\mathcal{C} = \begin{bmatrix} \vdots \\ (\eta_{i-1} - \eta_i)^\top (\eta_{i-1} - \eta_i) - r^2 \\ (\eta_i - \eta_{i+1})^\top (\eta_i - \eta_{i+1}) - r^2 \\ \vdots \\ (\eta n - \eta_1)^\top (\eta_n - \eta_1) - r^2 \end{bmatrix}.$$

The Lagrangian multiplier for constraint i, λ_i, depends only on vehicle i and $i+1$; similarly, λ_{i-1} depends on vehicle $i-1$ and i. According to (9), it follows that the control law for vehicle i only depends on its own and its neighbors' information.

Hence, there is no explicit leader or any exogenous system in this design and the controllers are implemented in a decentralized framework. For marine surface vessels, the link for communication channels is radio frequency.

B. Extension to Underactuated Ships

A common thruster configuration for marine surface vessels is rudder and propellers. Since the control vector's dimension is less than the degrees of freedom (DOFs), the vessel is underactuated and the lateral position cannot be directly controlled. For such a vessel the method proposed in Section II cannot be immediately applied to control the vessel's center of gravity. However, by controlling a point along the vessel's longitudinal axis, in the bow or ahead of the ship, the lateral position can be controlled indirectly. The authors of [41] stabilize an underactuated ship by locating a body-fixed coordinate system in the bow or ahead of the ship. The authors of [42] consider Lagrangian systems underactuated by one control, and characterize those systems that are configuration flat, i.e., equivalent to a fully actuated system. We proceed by showing how our formation control scheme can be extended to underactuated vessels.

Consider a ship and a point mass as in Fig. 3 where l is the length between point mass vessel's bow, subscript cg denotes the center of gravity, subscript q denotes the point mass, x_p is the length between bow and the center of gravity, and $\eta = [x_{cg}, y_{cg}, \psi]^\top$. The distance between the bow and the mass point satisfies

$$x_T^2 + y_T^2 = l^2$$

which is equal to the constraint function

$$\begin{aligned} \mathcal{C}_T(x_q, y_q, \eta) = &(x_q - x_{cg} + x_p \cos(\psi))^2 \\ &+ (y_q - y_{cg} + x_p \sin(\psi))^2 - l^2 \\ = &0. \end{aligned} \tag{26}$$

With a control law for the point mass and resultant force F_u, the vessel will follow according to (26). For a positive x_p, the forces at the vessel's center of gravity are only in the longitudinal direction and angular around (x_{cg}, y_{cg}). Since no lateral forces are used to control the ships motion, this corresponds to a surface vessel actuated by rudders and propellers only. This can further be extended to all vessels in the formation.

IV. Case Studies

To illustrate how constraint functions are implicitly used in a formation setup control scheme for marine surface vessels, we analyze some schemes from formation [43] and synchronization [21] control of marine craft. Second, we investigate how a set of constraints helps us to control a formation during the initial phase—*the formation assembling phase*. Further, we combine constraint functions for formation control and trajectory tracking for a single vessel. The result will be a group of vessels following a given trajectory in a specified configuration.

A. Control Plant Ship Model

The control plant model of a fully actuated tugboat in three DOFs: surge, sway, and yaw, is used in all the case studies. The model has been developed using Octopus SEAWAY for Windows [44] and the marine systems simulator (MSS) [45]. SEAWAY is a frequency-domain ship motions PC program, based on the linear strip theory. It calculates the wave-induced loads, motions, added resistance, and internal loads in six DOFs for displacement ships and yachts, barges, semisubmersibles, or catamarans, sailing in either regular or irregular waves. The MSS is a Matlab/Simulink library and simulator for marine systems. It includes models for ships, underwater vehicles, and floating structures. The library also contains guidance, navigation, and control blocks for real-time simulation.

Output from SEAWAY was used in the MSS to generate a 3-DOFs horizontal plane vessel model linearized for cruise speeds around $u = 5$ m/s with nonlinear viscous quadratic damping in surge. Furthermore, the surge mode is decoupled from the sway and yaw mode due to port/starboard symmetry. The model is valid for maneuvering at cruise speed 5 m/s. A nonlinear speed-dependent formulation for station-keeping ($u = 0$) and maneuvering up to $u = 0.35\sqrt{gL_{pp}} = 6.3$ m/s (Froude number 0.35) is derived in [46]. Each vessel in the formation is modelled with fully actuated dynamics, but an extension to underacted vessels as in Section III-B is possible. We further assume that all states are available for feedback.

The body-fixed equations of motion are given as $i = 1, 2, 3$

$$\dot{\eta}_i = R(\psi_i)\nu_i \tag{27a}$$

$$M_i\dot{\nu}_i + C_i\nu_i + D_i(\nu_i)\nu_i = \tau_{\text{constraint},i} + \tau_{\text{env}}. \tag{27b}$$

We assume that the first-order wave-induced motion (rapidly varying) is filtered out by a *wave filter* [29]. The slowly varying environmental forces due to wave, drift, wind, and currents are collected in τ_{env}. The damping matrix is written as the sum of linear and nonlinear terms, i.e., $D_i(\nu_i) = D_i + D_n(\nu_i)$. The numerical values are

$$M_i = \begin{bmatrix} 180.3 & 0 & 0 \\ 0 & 2.436 & 1.3095 \\ 0 & 1.3095 & 172.2 \end{bmatrix} \times 10^6$$

$$C_i = \begin{bmatrix} 0 & 0 & 0 \\ 0 & 0 & 8.61 \\ 0 & -8.61 & 0 \end{bmatrix} \times 10^6$$

$$D_i = \begin{bmatrix} 3.883 \times 10^{-9} & 0 & 0 \\ 0 & 0.2181 & -3.434 \\ 0 & 3.706 & 26.54 \end{bmatrix} \times 10^6$$

and $D_n(\nu_i) = \operatorname{diag}\left(-2.393 \times 10^{-3}\,|u_i|, 0, 0\right)$. The other model parameters are given as mass $m = 1\,722\,000$ kg, length $L_{pp} = 33$m, breadth $B = 9.45$ m, draught $T = 7.10$ m, center of gravity $CG = [-3,\ 0,\ 4.098]$ m, and center of buoyancy $CB = [-0.812,\ 0,\ 4.022]$ m with respect to keel line and $L_{pp}/2$. For the control design part, the matrices are transformed as in Section II-A.

B. Formation Control Schemes and Constraints

This section will show that, under some assumptions, constraint functions of the form discussed in this paper appear implicitly in some schemes for coordinated control of a group of ships.

In the formation design given in [43], the control objective is to force an error vector z to zero. The error vector contains information about both position and velocity, where the position error is defined as

$$z_{1i} = \eta_i - \xi_i, \qquad i = 1, 2$$

where $\eta_{1i} \in \mathbb{R}^n$ is the position and $\xi_i \in \mathbb{R}^n$ is the desired location for the ith member of the formation. Consider a formation with two members where $\xi_i = \xi + R(\psi)\, l_i$, $l_i \in \mathbb{R}^3$ for $i = 1, 2$ and assume that $R(\psi) = I$. This corresponds to a desired motion where the formation moves parallel to the x-axis in the inertial frame. When the systems have reached $z = 0$ the position errors are

$$\begin{aligned} z_{11} &= \eta_1 - \xi_1 = \eta_1 - \xi - l_1 = 0 \\ z_{12} &= \eta_2 - \xi_2 = \eta_2 - \xi - l_2 = 0. \end{aligned}$$

Combining z_{11} and z_{12} gives $\eta_1 - \xi - l_1 = \eta_2 - \xi - l_2$, or $\eta_1 - \eta_2 - (l_1 - l_2) = \eta_1 - \eta_2 - d_{12} = 0$. Similar with the velocity errors, $z_{2i} = \dot{\eta}_i - A_{1i}z_{1i}$. For the two systems, we obtain

$$\begin{aligned} z_{21} &= \dot{\eta}_1 - A_{11}(\eta_1 - \xi - l_1) = 0 \\ z_{22} &= \dot{\eta}_2 - A_{12}(\eta_2 - \xi - l_2) = 0 \end{aligned}$$

where $\dot{\eta}_i$ is the velocity and A_{1i} is a control design matrix. A combination of z_{21} and z_{22} gives (assuming that $A_{11} = A_{12}$)

$$\begin{aligned} \dot{\eta}_1 - A_{11}(\eta_1 - \xi - l_1) &= \dot{\eta}_2 - A_{12}(\eta_2 - \xi - l_2) \\ \dot{\eta}_1 - \dot{\eta}_2 &= A_{11}(z_{11} - z_{12}) = 0 \end{aligned}$$

and, hence, the error variable gives constraints on the form

$$\begin{aligned} \mathcal{C}(\eta) &= \eta_1 - \eta_2 - d_{12} = 0 \\ \dot{\mathcal{C}}(\eta) &= \dot{\eta}_1 - \dot{\eta}_2 = W(\eta)\dot{\eta} = 0. \end{aligned}$$

With the previous assumptions, we see that in the formation assembling phase, the set $\mathcal{M}$ corresponds to $\mathcal{M}_c$.

In [21], the authors use synchronization techniques to develop a control law for rendezvous control of ships. In a case study with two ships, the control objective is to control the supply ship to a position relative to the main ship. The desired configuration is reached when the errors $e = \eta_S - \eta_M$ and $\dot{e} = \dot{\eta}_S - \dot{\eta}_M$ are zero, where the subscripts S and M stands for supply ship and main ship, respectively. Both error functions fit into the framework for constraints in Section II-A.

For a replenishment operation, we define the constraint function to depend on the lateral position coordinate only. Then, the supply vessels converge to a position parallel to the course of the main ship, and this position is maintained during forward speed for replenishment purposes.

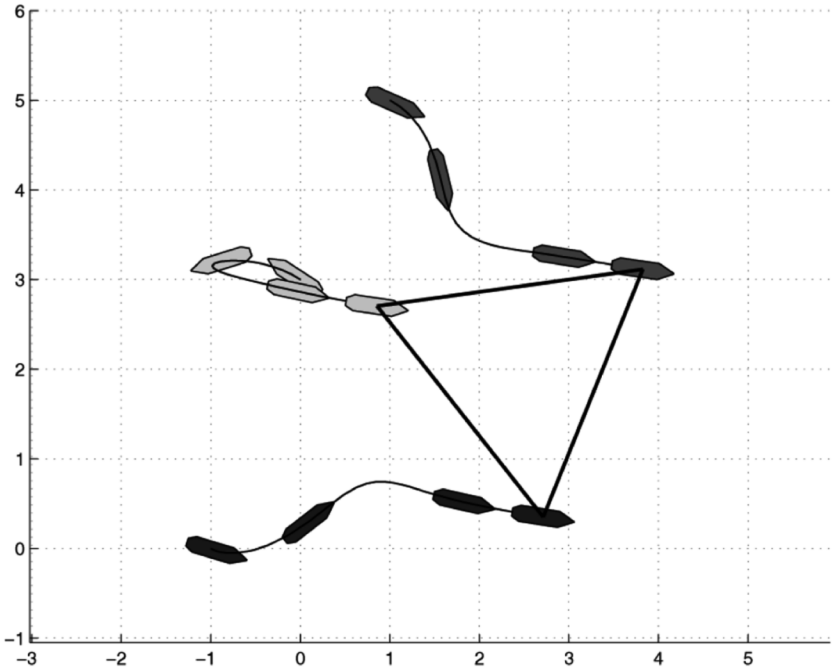

Fig. 4. Position of vessels during assembling. Uppermost vessel is the vessel 1 and the vessel 3 is at the bottom. Final configuration is shown with solid lines.

C. Case 1: Assembling of Marine Craft

We consider a formation of three vessels where the control objective is to assemble the craft in a predefined configuration, e.g., to be in position to tow a barge or another object. We assume there are no external forces acting on the formation, i.e., $\tau = 0$. The purpose is to show that assembling of the individual vessels into a formation can be done by imposing constraint functions.

Consider the constraint function

$$\mathcal{C}_1(\eta) = \begin{bmatrix} (x_1 - x_2)^2 + (y_1 - y_2)^2 - r_{12}^2 \\ (x_2 - x_3)^2 + (y_2 - y_3)^2 - r_{23}^2 \\ (x_3 - x_1)^2 + (y_3 - y_1)^2 - r_{31}^2 \end{bmatrix} = 0 \qquad (28)$$

where $x_i, y_i \in \mathbb{R}$ is the position vector in the Earth-fixed reference frame and $r_{ij} \in \mathbb{R}$ is the distance between vessel i and j. This constraint enables us to specify the positions of each vessel with respect to the others. The constraint manifold is equivalent to the formation configuration, and by the previous sections, we know that $\mathcal{M}_c$ is stabilized using feedback from the constraints. Hence, the proposed approach gives the control laws for formation assembling. From the ship model (27) and the constraint (28), we have

$$M_\eta \ddot{\eta} + n(\nu, \eta, \dot{\eta})\dot{\eta} = -R(\psi)W_1(\eta)^\top \lambda \qquad (29)$$

where $M_\eta = M_\eta(\eta) = \mathrm{diag}\,(M_{\eta 1}, M_{\eta 2}, M_{\eta 3})$, $\eta = \left[\eta_1^\top, \eta_2^\top, \eta_3^\top\right]^\top$, and so on. Further, the Lagrangian multiplier is obtained from

$$W_1 M_\eta^{-1} R W_1^\top \lambda = -W_1 M_\eta^{-1} n(\nu, \eta, \dot{\eta})\dot{\eta} + \dot{W}_1(\eta)\dot{\eta} + K_d \dot{\mathcal{C}}_1(\eta) + K_p \mathcal{C}_1(\eta). \qquad (30)$$

The control parameters chosen to stabilize the constraint function $\mathcal{C}_1$ are $K_p = 1.6 I_3$ and $K_d = 0.64 I_3$, the formation is defined by $r_{12} = 2$, $r_{23} = 3$, and $r_{31} = 3$, and the vessels start in $\eta_{10} = [1, 5, 0]^\top$, $\eta_{20} = [0, 3, 0]$, and $\eta_{30} = [-1, 0, 0]$—all with zero initial velocity.

Fig. 4 shows position response during assembling. The time plots of the constraint function $\mathcal{C}_1$ and its time derivative $W_1(\eta)\nu$ are shown in Fig. 5. The constraints and velocity terms converge to zero, and the constraint manifold is reached. The vessels have converged to the nearest positions where the constraints are fulfilled, and the formation is hence assembled in the desired configuration.

D. Case 2: Assembling and Point Stabilization

Equation (28) gives the configuration of the formation, but with no specified location on the sea surface. If the control objective is to assemble the formation and position the first vessel in a desired location, we add a row to (28), such that

$$\mathcal{C}_{1b}(\eta) = \begin{bmatrix} (x_1 - x_2)^2 + (y_1 - y_2)^2 - r_{12}^2 \\ (x_2 - x_3)^2 + (y_2 - y_3)^2 - r_{23}^2 \\ (x_3 - x_1)^2 + (y_3 - y_1)^2 - r_{31}^2 \\ \eta_1 - \eta_{\mathrm{des}} \end{bmatrix} = 0 \qquad (31)$$

where $\eta_{\mathrm{des}} \in \mathbb{R}^3$ is the fixed desired position and orientation. To demonstrate performance of the proposed controller, the ships are subject to environmental disturbances, unmeasured biases b, and white noise w. Further, communication is constrained by time delays in the links between each ship. The ship model (27) and the constraint (31) give the equation of motion:

$$M_\eta \ddot{\eta} + n(\nu, \eta, \dot{\eta})\dot{\eta} = b + R^\top(\psi)w - R(\psi)W_{1b}(\eta)^\top \lambda. \qquad (32)$$

Since b and w are assumed to be unknown, the Lagrangian multiplier is obtained as in (30). The last addition in the constraint function is equal to a PD-controller for the first vessel, so (31) leads to a combination of a formation controller and a PD-type-controller for dynamic positioning of ships [29]. Hence, several control laws are handled in one step using the proposed approach.

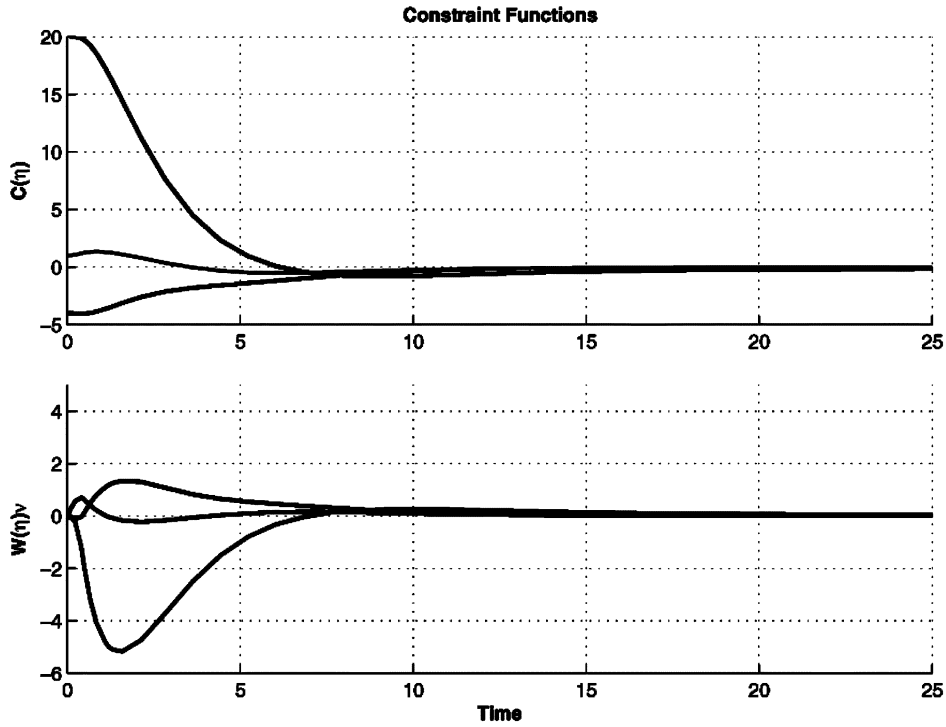

Fig. 5. Response of assembling constraints.

The control parameters chosen to stabilize the constraint function $\mathcal{C}_{1b}$ are $K_p = 0.4I_3$ and $K_d = 0.04I_3$. The desired position for the first vessel is $\eta_{\text{des}} = [2, 3, 0]^\top$ while the desired formation configuration, initial position, and velocity are the same as before. All communication links have a 2-s delay, and the unknown environmental disturbances are chosen as $b = \left[10^4, 0, 0\right]$ for each vessel. In addition, the states are affected by white noise.

The addition of the last vector row in $\mathcal{C}_{1b}$ adds three more signals, the error vector $\tilde{\eta} = \eta_1 - \eta_{\text{des}}$, to the constraint function, shown in Fig. 7. As seen in Fig. 6, the vessels assemble according to the constraints, but this time vessel 1 is positioned at its desired position η_{des}. This, together with the unknown bias, forces the two other vessels to move to a different position compared to the first case to satisfy the constraint. As time evolves, the constraint function $\mathcal{C}_2$ and derivative $W_2(\eta)\nu$ tend to zero, and the formation is assembled in its proper configuration with vessel 1 in the desired location.

E. Case 3: Combined Trajectory Tracking and Formation Control

A combination of trajectory tracking for a vessel and relative distance constraint functions is interesting for an application where it is required that one vessel follows a predefined path while the other members of the formation follow that vessel in a certain distance. This case is described by the constraint function

$$\mathcal{C}_2(\eta, t) = \begin{bmatrix} (x_1 - x_2)^2 + (y_1 - y_2)^2 - r_{12}^2 \\ (x_2 - x_3)^2 + (y_2 - y_3)^2 - r_{23}^2 \\ (x_3 - x_1)^2 + (y_3 - y_1)^2 - r_{31}^2 \\ \eta_1 - \eta_d(t) \end{bmatrix} = 0$$

where $\eta_d(t) \in \mathbb{R}^3$ is the desired position and orientation at time t. It is straightforward to show that the origin $\mathcal{C}_2(\eta, t) = 0$ is uniformly globally exponentially stable in the presence of zero disturbances with the approach in Section II-B.

The desired path is given by

$$\eta_d(t) = \begin{bmatrix} x_d(t) \\ y_d(t) \\ \psi_d(t) \end{bmatrix} = \begin{bmatrix} t \\ A \sin \omega t \\ \text{atan2}\left(\dfrac{\dot{y}_d}{\dot{x}_d}\right) \end{bmatrix}$$

where the atan2-function is used to ensure correct mapping of the heading angle into $[-\pi, \pi]$. The initial values for the vessels are $\eta_1 = [0, 0, \pi/2]^\top$, $\eta_2 = [0, 4, \pi/2]^\top$, $\eta_3 = [-4, 0, \pi/2]^\top$, and $\nu_{1,2,3} = 0$. The path is defined by $A = 10$ and $\omega = 0.04$, while the formation is shaped according to $r_{12} = r_{31} = 5$ and $r_{23} = 3$. The controller gains are $(I = I_3)$, for the trajectory tracking constraint $K_p = 2I$ and $K_d = 2I$, and for the formation keeping constraints $K_p = 3.6$ and $K_d = 9$.

Fig. 8 shows the position of the three vessels in the formation while vessel 1 is tracking the desired trajectory $\eta_d(t)$. The constraint functions tend to zero in Fig. 9, where the upper part shows the constraints related to the formation configuration, and the lower part shows the tracking error. Vessel 1 tracks the desired trajectory while vessels 2 and 3 follow in a triangular shape according to the formation configuration. Note that no collisions occur when the formation constraints are met.

The simulations in this section have only considered constraint functions that lead to the triangular formations, but depending on the number of constraint functions and members in the formation, the formation can be configured in many different ways, e.g., line- (in the transversal or longitudinal direction), circle-, or box-shaped, by changing the constraint function as discussed in Section II-D.

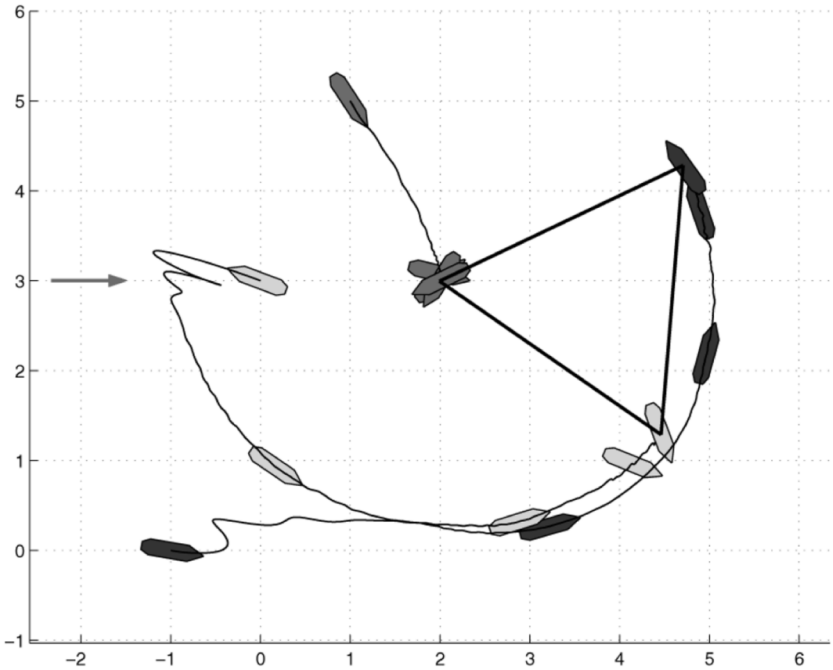

Fig. 6. Position of vessels during assembling while vessel 1 is positioned at $\eta_{\text{des}} = [2, 3, 0]^\top$. The arrow is the unknown bias. Final configuration is shown as a solid line.

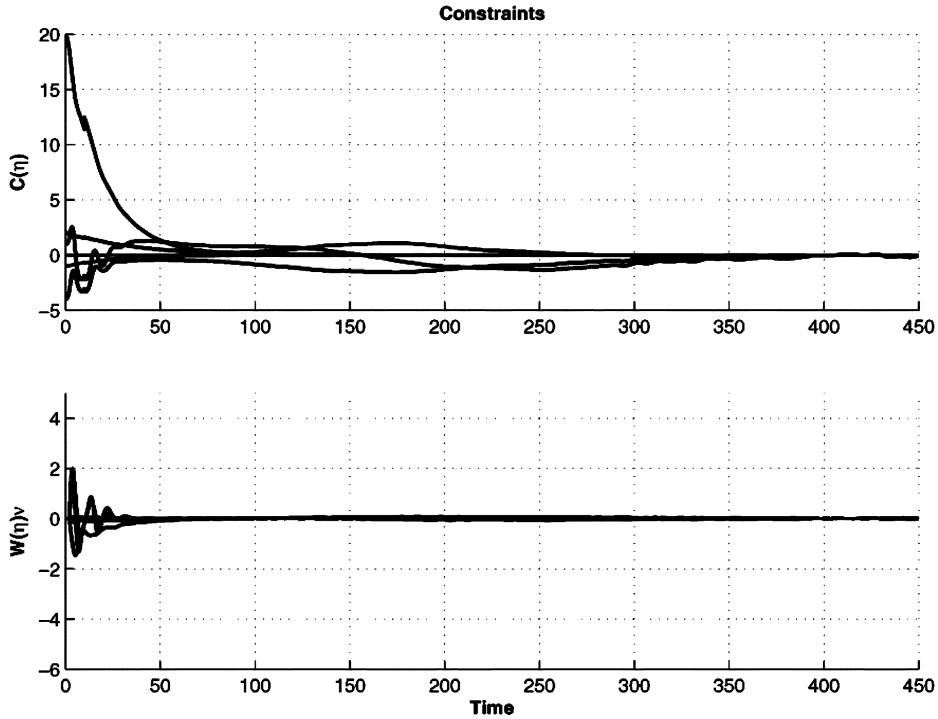

Fig. 7. Time response of assembling and PD constraints.

For simplicity, this paper has only considered holonomic constraint functions between different vehicles, i.e., kinematic constraints which can be expressed as finite relations between the generalized coordinates. However, the suggested approach can be extended to nonholonomic intervessel constraints which are linear in the generalized velocities as shown in [47].

V. Concluding Remarks

In this paper, we have shown how individual ships can be controlled as a formation by designing constraint functions that force the vessels to assemble and remain in a desired configuration. The functions are maintained by constraint forces on the individual vehicles which arise due to the imposed constraints.

The constraint forces, which are interpreted as control laws, are derived in an analytical setting using Lagrangian multipliers. Furthermore, feedback from the constraints is used to render the system robust against initial position errors during formation assembling, external disturbances, and measurement noise. The resulting formation constraint forces are nonzero only when the constraints are violated—when the constraint is fulfilled, the

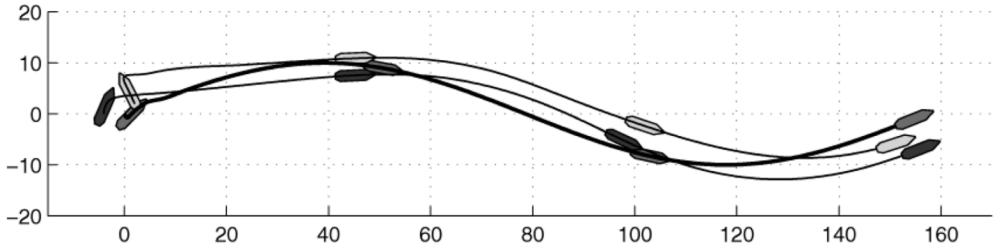

Fig. 8. Position plot of the three vessels in a constrained formation during trajectory tracking. The bold line is vessel 1 following the desired trajectory $\eta_d\,(t)$.

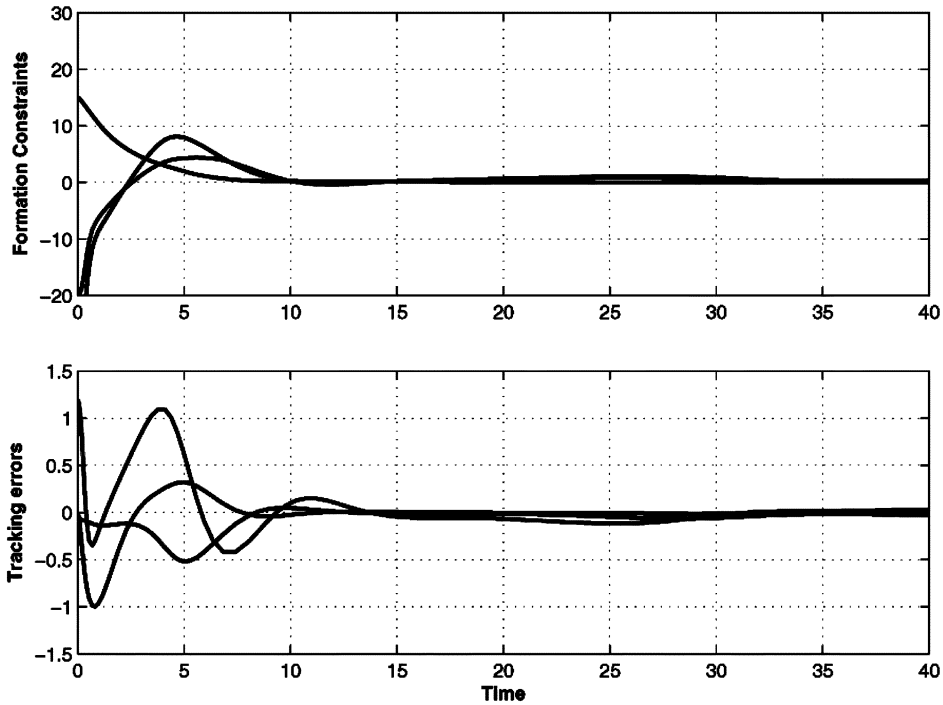

Fig. 9. Constraint responses during the first 40 s of the simulation. The upper plot shows formation errors and the lower plot shows $\eta - \eta_d\,(t)$.

corresponding multiplier and constraint force is zero. Furthermore, the same approach has been applied with no major modification to control purposes.

In particular, we have come up with control laws which maintain the formation structure and our approach can be used to combine control laws to simultaneously achieve desired behavior and maintain formation configuration. Furthermore, we have seen how constraints appear in different control schemes for multiple marine craft. Applications have been illustrated by simulations of formation of marine craft where robustness with respect to unknown biases, time delays, and white noise.

ACKNOWLEDGMENT

The authors would like to thank F. Arrichello, J.-J. Slotine, and the reviewers for their comments that improved the presentation of the manuscript.

REFERENCES

[1] A. Okubo, "Dynamical aspects of animal grouping: Swarms, schools, flocks, and herds," *Adv. Biophys.*, vol. 22, pp. 1–94, 1986.

[2] B. L. Partridge, "The structure and function of fish schools," *Sci. Amer.*, pp. 90–99, Jun. 1982.

[3] J. K. Parrish and L. Edelstein-Keshet, "Complexity, pattern, and evolutionary trade-offs in animal aggregation," *Science*, vol. 284, no. 5411, pp. 99–101, 1999.

[4] V. Kumar, N. Leonard, and A. S. Morse, Eds., "Cooperative Control," in *Lecture Notes in Control and Information Sciences*. Berlin, Germany: Springer-Verlag, 2005, vol. 309.

[5] C. W. Reynolds, "Flocks, herds, and schools: A distributed behavioral model," *Comput. Graphics Proc.*, vol. 21, no. 4, pp. 25–34, 1987.

[6] ——, Boids (2001) [Online]. Available: http://www.red3d.com/cwr/boids/

[7] P. Ögren, E. Fiorelli, and N. E. Leonard, "Cooperative control of mobile sensor networks: Adaptive gradient climbing in a distributed environment," *IEEE Trans. Autom. Control*, vol. 49, no. 8, pp. 1292–1302, Aug. 2004.

[8] T. B. Curtin and J. G. Bellingham, "Guest editorial—Autonomous ocean-sampling networks," *IEEE J. Ocean. Eng.*, vol. 26, no. 4, pp. 421–423, Oct. 2001.

[9] D. A. Schoenwald, "Auvs: In space, air, water, and on the ground," *IEEE Control Syst. Mag.*, vol. 20, no. 6, pp. 15–18, Dec. 2000.

[10] J. A. Fax and R. M. Murray, "Information flow and cooperative control of vehicle formations," *IEEE Trans. Autom. Control*, vol. 49, no. 9, pp. 1465–1476, Sep. 2004.

[11] R. W. Beard, J. Lawton, and F. Y. Hadaegh, "A coordination architecture for spacecraft formation control," *IEEE Trans. Control Syst. Technol.*, vol. 9, no. 6, pp. 777–790, Nov. 2001.

[12] A. Jadbabaie, J. Lin, and A. S. Morse, "Coordination of groups of mobile autonomous agents using nearest neighbor rules," *IEEE Trans. Autom. Control*, vol. 48, no. 6, pp. 988–1101, Dec. 2002.

[13] P. K. C. Wang, "Navigation strategies for multiple autonomous robots moving in formation," *J. Robot. Syst.*, vol. 8, no. 2, pp. 177–195, 1991.

[14] P. Encarnação and A. Pascoal, "Combined trajectory tracking and path following: An application to the coordinated control of autonomous marine craft," in *Proc. 40th IEEE Conf. Decision Control*, Orlando, FL, 2001, pp. 964–969.

[15] T. Balch and R. C. Arkin, "Behavior-based formation control for multirobot teams," *IEEE Trans. Robot. Autom.*, vol. 14, no. 6, pp. 926–939, Dec. 1998.

[16] W. Ren and R. W. Beard, "Formation feedback control for multiple spacecraft via virtual structures," *IEE Proc. Control Theory Appl.*, vol. 151, no. 3, pp. 357–368, 2004.

[17] M. Egerstedt and X. Hu, "Formation constrained multi-agent control," *IEEE Trans. Robot. Autom.*, vol. 17, no. 6, pp. 947–951, Dec. 2001.

[18] B. Siciliano and J.-J. E. Slotine, "A general framework for managing multiple tasks in highly redundantrobotic system," in *Proc. 5th Int. Conf. Adv. Robot.*, Pisa, Italy, 1991, pp. 1211–1216.

[19] D. J. Stilwell and B. E. Bishop, "Redundant manipulator techniques for a path planning and control of a platoon of autonomous vehicles," in *Proc. 41st IEEE Conf. Decision Control*, Las Vegas, NV, 2002, pp. 2093–2098.

[20] G. Antonelli and S. Chiaverini, "Fault tolerant kinematic control of platoons of autonomous robots," in *Proc. IEEE Int. Conf. Robot. Autom.*, New Orleans, LA, 2004, pp. 3313–3318.

[21] E. Kyrkjebø and K. Y. Pettersen, "Ship replenishment using synchronization control," in *Proc. 6th IFAC Conf. Manoeuvring Control Marine Crafts*, Girona, Spain, 2003, pp. 286–291.

[22] I.-A. F. Ihle, R. Skjetne, and T. I. Fossen, "Nonlinear formation control of marine craft with experimental results," in *Proc. 43rd IEEE Conf. Decision Control*, Atlantis, the Bahamas, 2004, pp. 680–685.

[23] C. Lanczos, *The Variational Principles of Mechanics*, 4th ed. New York: Dover, 1986.

[24] I.-A. F. Ihle, J. Jouffroy, and T. I. Fossen, "Formation control of marine surface craft using Lagrange multipliers," in *Proc. 44rd IEEE Conf. Decision Control and 5th Euro. Control Conf.*, Seville, Spain, 2005, pp. 752–758.

[25] J. L. Lagrange, "Mécanique analytique, nouvelleédition," in *Académie Des Sciences, 1811*. Norwell, MA: Kluwer, 1997, Translated Version: *Analytical Mechanics*.

[26] D. Baraff, "Linear-time dynamics using lagrange multipliers," *Comput. Graphics Proc. SIGGRAPH*, pp. 137–146, 1996.

[27] R. Barzel and A. H. Barr, "A modeling system based on dynamic constraints," *Comput. Graphics*, vol. 22, no. 4, pp. 179–188, 1988.

[28] R. Bhatt and V. Krovi, "Comparison of alternate methods for distributed motion planning of robot collectives within a potential field framework," in *Proc. IEEE Int. Conf. Robot. Autom.*, Barcelona, Spain, 2005, pp. 99–104.

[29] T. I. Fossen, *Marine control systems: Guidance, navigation and control of ships, rigs and underwater vehicles*. Trondheim, Norway: Marine Cybernetics, 2002 [Online]. Available: http://www.marinecybernetics.com

[30] D. C. Tarraf and H. H. Asada, "On the nature and stability of differential-algebraic systems," in *Proc. Amer. Control Conf.*, Anchorage, AK, 2002, pp. 3546–3551.

[31] L. Petzold, "Differential/algebraic equations are not ODEs," *SIAM J. Sci. Stat. Comput.*, vol. 3, no. 3, pp. 367–384, 1982.

[32] A. A. T. Dam, "Stable numerical integration of dynamical systems subject to equality state-space constraints," *J. Eng. Math.*, vol. 26, pp. 315–337, 1992.

[33] H. Khalil, *Nonlinear Systems*, 3rd ed. New York: Prentice-Hall, 2002.

[34] J. Baumgarte, "Stabilization of constraints and integrals of motion in dynamical systems," *Comput. Methods Appl. Mech. Eng.*, vol. 1, pp. 1–16, 1972.

[35] L. R. Petzold, Y. Ren, and T. Maly, "Regularization of higher-index differential-algebraic equations with rank-deficient constraints," *SIAM J. Sci. Stat. Comput.*, vol. 18, no. 3, pp. 753–774, 1997.

[36] H. Krishnan and N. H. McClamroch, "Tracking in nonlinear differential-algebraic control systems with applications to constrained robot systems," *Automatica*, vol. 30, no. 12, pp. 1885–1897, 1994.

[37] N. H. McClamroch and D. Wang, "Feedback stabilization and tracking of constrained robots," *IEEE Trans. Autom. Control*, vol. 33, no. 5, pp. 419–426, May 1988.

[38] X. Yun and N. Sarkar, "Unified formulation of robotic systems with holonomic and nonholonomic constraints," *IEEE Trans. Robot. Autom.*, vol. 14, no. 4, pp. 640–650, Aug. 1998.

[39] A. Maciejewski and C. Klein, "Numerical filtering for the operation of robotic manipulators through kinematically singular configurations," *J. Robot. Syst.*, vol. 5, pp. 527–552, 1988.

[40] S. Chiaverini, B. Sicilliano, and O. Egeland, "Review of the damped least-squares inverse kinematics with experiments on an industrial robot manipulator," *IEEE Trans. Control Syst. Technol.*, vol. 2, no. 2, pp. 123–134, Jun. 1994.

[41] T. I. Fossen, J. M. Godhavn, S. P. Berge, and K. P. Lindegaard, "Nonlinear control of underactuated ships with forward speed compensation," in *Proc. 4th IFAC Nonlinear Control Syst. Design Symp. (NOLCOS)*, Enschede, The Netherlands, 1998, pp. 121–127.

[42] M. Rathinam and R. M. Murray, "Configuration flatness of Lagrangian systems underactuated by one control," *SIAM J. Control Optim.*, vol. 36, no. 1, pp. 164–179, 1998.

[43] R. Skjetne, S. Moi, and T. I. Fossen, "Nonlinear formation control of marine craft," in *Proc. 41st IEEE Conf. Decision Control*, Las Vegas, NV, 2002, pp. 1699–1704.

[44] Amarcon B. V., "Octopus Seaway" The Netherlands, 2005 [Online]. Available: http://www.amarcon.com

[45] Norwegian Univ. Sci. Technol., "Marine Systems Simulator (MSS)" Trondheim, Norway, 2005 [Online]. Available: http://www.cesos.ntnu.no/mss

[46] T. I. Fossen, "A nonlinear unified state-space model for ship maneuvering and control in a seaway," *Int. J. Bifurcation Chaos*, vol. 15, no. 9, pp. 2717–2746, 2005.

[47] I. R. Gatland, "Nonholonomic constraints: A test case," *Amer. J. Phys.*, vol. 72, no. 7, pp. 941–942, Jul. 2004.